

1 **Carbon, nitrogen, and sulphur isotope analysis of the Padanian Plain sediments: backgrounds**
2 **and provenance indication of the alluvial components**

3 Salani G.M.¹, Brombin V.^{1,2}, Natali C.³, Bianchini G.^{1,2*}

4

5 ¹ Department of Physics and Earth Sciences, University of Ferrara, 44122 Ferrara, Italy;

6 ² Institute of Environmental Geology and Geoengineering of the Italian National Research Council
7 (CNR-IGAG), 00015 Montelibretti, Italy;

8 ³ Department of Earth Sciences, University of Florence, 50121 Florence, Italy.

9

10 **Abstract**

11 This work reports an *ab initio* study on the carbon (C), nitrogen (N), and sulphur (S) elemental and
12 isotope compositions of the Padanian Plain sediments collected in the province of Ferrara (Northern
13 Italy). The investigated sediments were already characterized by previous research that highlighted a
14 bimodal provenance, as some sediments are from the Alpine chain and were conveyed to the plain by
15 Po River, whereas others are from the Apennine chain and were conveyed to the plain by the Reno
16 River. This information was obtained considering the concentration of heavy metals retrieved from
17 hundreds of X-ray fluorescence analyses available in the literature, whereas CNS elemental and
18 isotope compositions are unknown. These tracers are generally considered scarcely useful to identify
19 the sediment source areas, as influenced by multiple environmental factors. However, this work
20 challenges these assertions observing that $^{13}\text{C}/^{12}\text{C}$, $^{15}\text{N}/^{14}\text{N}$, $^{34}\text{S}/^{32}\text{S}$ are significantly different in Po
21 and Reno River sediments. Our hypothesis is that the CNS geochemical signal is 1) mainly regulated
22 by the organic fraction included in the alluvial sediments, and 2) these organic fraction has in turn a
23 specific composition in the distinct source catchments. More in general, the presented data increase
24 knowledge on the local elemental and isotopic backgrounds. This is important because many
25 pollutants contain significant CNS concentration and specific isotope composition. Therefore, they

26 serve as baseline and will provide new tools to recognize possible anthropogenic anomalies in the
27 studied area.

28

29 **Keywords:** CNS isotopes, alluvial sediments, Padanian Plain, Po River, Reno River, isotopic
30 fractionation, biogeochemical processes

31

32 **1. Introduction**

33 The geochemical signatures of sediments in alluvial plains record the geochemistry of the parent
34 rocks and the weathering mechanisms occurred in the source areas. However, geochemical signatures
35 are often complex to be interpreted because distinct rivers (and tributaries) drain geologically
36 different sub-basins, sometimes conveying different sediments in the same alluvial plain. In general,
37 major and trace elements are used to trace the sediments' provenance as they reflect the source rock
38 composition (Bianchini et al., 2012; Balabanova et al., 2016; Nyobe et al., 2018; Salomão et al., 2020;
39 Vicente et al., 2021). However, secondary pedological processes, related to the local climatic
40 conditions could affect the primary signature (Costantini et al., 2002; Caporale and Violante, 2016).
41 In addition, the natural (geogenic) geochemical fingerprint of the alluvial sediments can be
42 overprinted by anthropogenic contributions in agricultural, industrial, and urban areas (Galán et al.,
43 2014; Barbieri et al., 2018). Therefore, in order to better constrain the sources of alluvial sediments,
44 new geochemical proxies have to be tested to delineate the provenance of sediments and features of
45 the relative depositional environments. Among the various case-studies, alluvial sediments in the
46 province of Ferrara, located in the easternmost sector of the Padanian Plain (Northern Italy), have
47 been widely studied from the geochemical point of view (Amorosi et al., 2002; Amorosi, 2012;
48 Bianchini et al., 2012; 2013, 2019; Di Giuseppe et al., 2014a; 2014b; 2014c). The soils of this specific
49 sector of the plain are composed by young (Holocene in age) alluvial deposits transported by Po and
50 Reno fluvial systems. Previous investigations on these sediments were mainly focused on major
51 elements having lithophile affinity (Si, Al, Ti, Fe, Mn, Mg, Ca, Na, K, P) and heavy metals (Ni, Co,

52 Cr, V, Sc, Cu, Pb, Zn) to constrain the distribution of potentially toxic elements (Di Giuseppe et al.,
53 2014a; 2014b; 2014c, Bianchini et al., 2012; 2013; 2019). They were important to define the local
54 geochemical backgrounds, as well as the sediments provenance, *i.e.*, which fluvial system conveyed
55 its alluvial load in the plain (Bianchini et al., 2012). In particular, specific trace element such as nickel
56 (Ni) and chromium (Cr) were effective in discriminating between alluvial sediments from Po and
57 Reno Rivers, the two fluvial systems that are interacting in the area (Bianchini et al., 2012; 2013;
58 2019). In fact, the Po River sediments are richer in Ni and Cr than Reno River sediments, because the
59 parent rocks outcropping in the Po River catchment include mafic and ultramafic lithologies rich in
60 heavy metals (Amorosi, 2012). In the above-mentioned studies essential elements such as carbon (C),
61 nitrogen (N), and sulphur (S) have been scarcely investigated, and information on their isotopic ratios
62 ($^{13}\text{C}/^{12}\text{C}$, $^{15}\text{N}/^{14}\text{N}$, $^{34}\text{S}/^{32}\text{S}$) is missing. The stable isotope compositions of C, N, and S of soils and
63 sediments vary significantly, reflecting the nature of the parent rock material, the current and past
64 climates and vegetation, and the effects of other organisms (Anderson, 1988). Therefore, they could
65 be used as additional proxies to trace the source areas of the weathered material, which was mobilized
66 by erosion, transported by rivers in the catchments and finally deposited in alluvial plains.

67 In order to test the effectiveness of CNS elemental and isotopic data in the provenance analysis,
68 sediment samples were selected from the collections of previous geochemical studies that emphasized
69 the origin of Padanian alluvial sediments on the basis of Ni and Cr content (Bianchini et al., 2012;
70 2013; Di Giuseppe et al., 2014a; 2014b; 2014c). This new investigation deals with the analysis of the
71 elemental and isotopic composition of C, N, and S of selected sample sediments having “Po affinity”
72 (*i.e.*, high Ni-Cr contents) and “Reno affinity” (*i.e.*, low Ni-Cr contents). The goal is to define CNS
73 elemental and isotopic backgrounds and to verify if these tracers can be used as additional proxies to
74 define the sediment provenance.

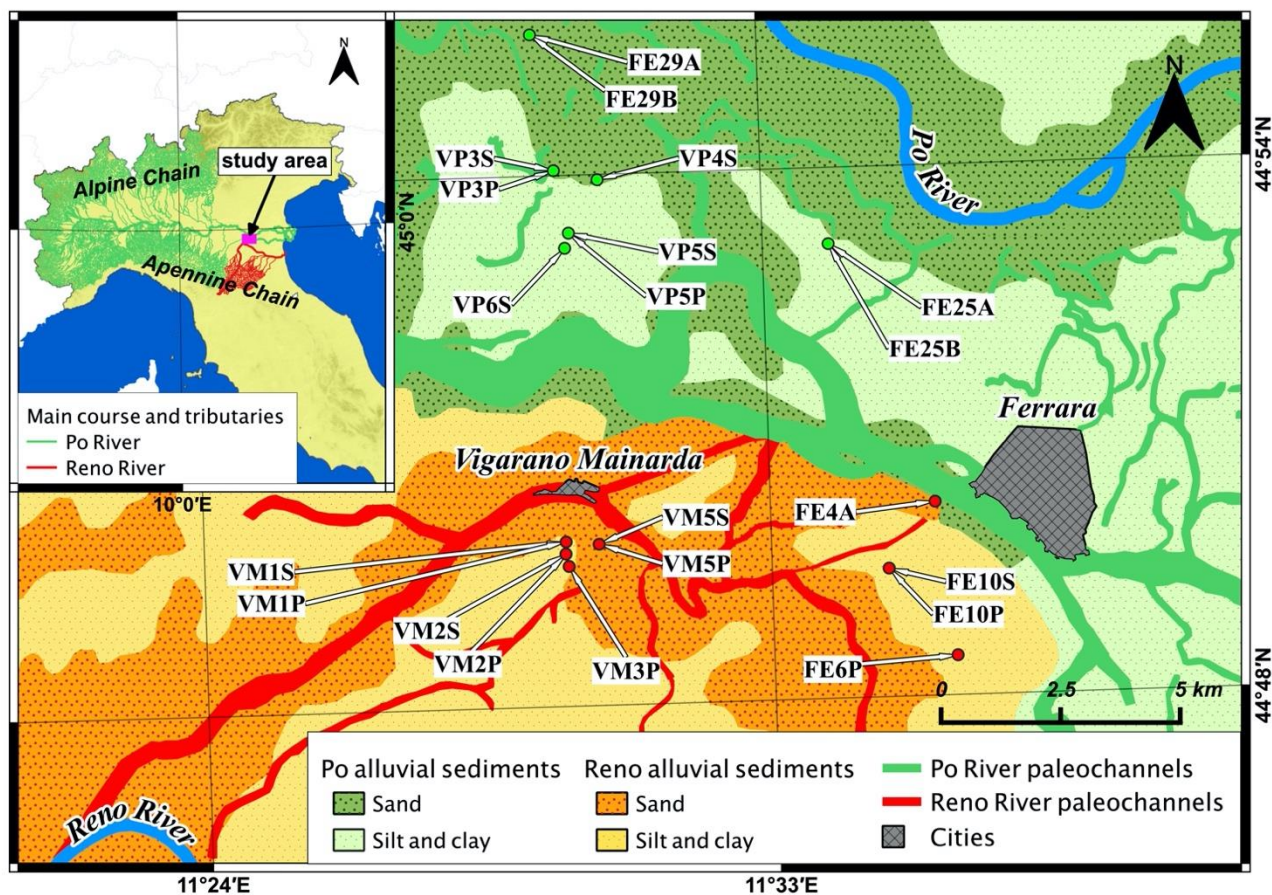
75

76 **2. Study area**

77 The Padanian Plain is the widest alluvial plain (~ 48,000 km²) of the Italian peninsula (Campo et al.,
78 2020). It is the morphological expression of the homonymous basin, which is bounded by the Alpine
79 and Apennine chains, at north and south respectively (Fig. 1a). The plain was characterized by marine
80 sedimentation in Pliocene to Early Pleistocene before progradation of fluvial sediments that was
81 enhanced during glaciation periods (Amorosi et al., 2019; 2021; Campo et al., 2020). The easternmost
82 part of the plain, where the Ferrara province is located, received sedimentary contributes from i) the
83 Po River, which is the principal Italian fluvial system crossing from west to east the Padanian Plain
84 with numerous tributaries from distinct parts of the Alps and the north-western Apennines (Marchina
85 et al., 2015; 2016; 2018), and ii) several torrents flowing from the north-eastern Apennines (Fig. 1;
86 Bianchini et al., 2002; 2012; 2014).

87 The sediments of Po River mainly derive from the western and central Alps and north-western
88 Apennines, where limestones, sandstones, as well as mafic and ultramafic rocks (*i.e.*, ophiolites) crop
89 out (Amorosi et al., 2002). On the other hand, sediments from north-eastern Apenninic rivers derive
90 from Cretaceous to Pliocene sedimentary rocks, such as sandstones, marls, and evaporites (Amorosi
91 et al., 2002; Manzi et al., 2007).

92 In particular, this study focused on the geochemistry of agricultural soils collected close to i) the town
93 of Ferrara (labels FE, F), and ii) the nearby village of Vigarano Mainarda (labels VM, VP). These
94 soils developed from alluvial sediments (sand, silt and clay carried by the Po and Reno Rivers) that
95 have been geochemically characterized by Bianchini et al. (2012; 2013). In these studies, the Po or
96 Reno related provenance of each sediment sample was identified based on their Ni and Cr contents.



97

98 **Figure 1.** Sedimentological map (modified from Bertolini et al., 2009) of the study area reporting the paleochannels and
 99 the location of the sediment samples. Samples collected near Ferrara are labelled FE, F; samples collected near Vigarano
 100 Mainarda are labelled VM, VP. The inset reports the location of the study area in Northern Italy and the main courses and
 101 tributaries of the Po and Reno fluvial systems.

102

103 3. Materials and methods

104 3.1. Sample selection

105 Ten sediment samples with “Po affinity” and eleven sediment samples with “Reno affinity” were
 106 selected. The samples were collected at two distinct depths: one representative of the plough horizon
 107 (just beneath the roots zone, at a depth of 30–40 cm) and the other representative of the underlying
 108 undisturbed layer (at a depth of 100–120 cm). The samples were powdered and homogenized within
 109 an agate mill before to proceed with further analyses.

110

111 3.2 C, N, S elemental and isotopic composition

112 The analyses of C, N, S contents (expressed in wt%) and the relative isotope ratios ($^{13}\text{C}/^{12}\text{C}$, $^{15}\text{N}/^{14}\text{N}$,
 113 $^{34}\text{S}/^{32}\text{S}$) were carried out at the Department of Physics and Earth Science of University of Ferrara

114 (Italy) using an elemental analyser (EA) Vario PYRO Cube (Elementar) operating in combustion
115 mode and coupled with the isotope ratio mass spectrometer (IRMS) precisiON (Elementar).
116 Homogenous powdered samples (around 40 mg) were weighed in tin capsules, wrapped, and finally
117 loaded in the EA autosampler to be analyzed.

118 The Vario PYRO Cube consists of a combustion oven operating at 1150°C. After the sample has been
119 burnt, the released C, N, and S gaseous species are transferred in a reduction column operating at
120 850°C that contains chips of native copper to reduce the nitrogen oxides (NO_x) to N₂. The analyte
121 gases pass into the original purge and trap module before to enter in the IRMS. Only N₂ is not trapped
122 and is introduced directly in the IRMS to be analyzed for isotopic composition determination. CO₂
123 and SO₂ are trapped respectively in two distinct traps. When the N isotopic analysis terminated, the
124 CO₂ trap is heated at 110°C to release CO₂ which flows in the IRMS to start the isotopic C analyses.
125 After that, the SO₂ trap is heated at 220°C to release the gas.

126 In the mass spectrometer the molecules of the sample gas are ionized by the source (*i.e.*, a thorium
127 oxide filament), and the ions pass through a magnet, which deflects and sorts them into beams with
128 distinctive mass/charge ratios (*m/z*). Then ion beams arrive at the collector where three Faraday cups
129 detect the ions of each of the three different masses of analyzed gas simultaneously (*i.e.*, for N₂ the
130 masses 28, 29, and 30, for CO₂ the masses are 44, 45, and 46 and for SO₂ the masses 64 and 66).

131 The detection of the distinct isotopic masses of the sample is bracketed between those of reference
132 gases (N₂, CO₂, SO₂, 5 grade purity), which have been calibrated using reference materials. In the
133 cups, the impact of the ions is translated into a recordable electrical signal, forming peaks, which area
134 is proportional to the number of incident ions. The isotope ratios are calculated through peak
135 definition and integration through the ionOS software.

136 The signal intensity is amplified by an integrated Amplifier and is expressed in nano-ampere (nA).
137 The signal intensity is referred as “peak height”, and the minimum acceptable signal is 1 nA (optimum
138 between 2 and 10 nA) in amplitude and at least 5 seconds in duration.

139 Additional data on the distinct carbon fractions (organic carbon, OC; inorganic carbon IC) were
140 carried out with the EA Vario MICRO cube coupled with the IRMS Isoprime100 (Elementar),
141 following the thermal speciation analytical approach defined by Natali et al. (2018).

142 Calibration of the instruments were performed using several standards: the limestone JLs-1 (Kusaka
143 and Nakano, 2014), the Carrara Marble (Natali and Bianchini, 2015), the Jacupiranga carbonatite
144 (Beccaluva et al., 2017), the peach leaves NIST SRM1547 (Dutta et al., 2006), the caffeine IAEA-
145 600, the Tibetan human hair powder USGS42 (Coplen and Qi, 2011), the Barium Sulfate IAEA-SO-
146 5 (Halas and Szaran, 2001).

147 The $^{13}\text{C}/^{12}\text{C}$, $^{15}\text{N}/^{14}\text{N}$, $^{34}\text{S}/^{32}\text{S}$ isotopic ratios (R) were expressed with the δ notation (in ‰ units):

$$148 \quad \delta = (R_{\text{sam}}/R_{\text{std}} - 1) \times 1000$$

149 where R_{sam} is the isotopic ratio of the sample and R_{std} is the isotopic ratio of the international isotope
150 standards Pee Dee Belemnite (PDB), air N_2 , and Canyon Diablo troilite (CDT) for C, N, and S
151 respectively.

152 Analytical uncertainties (1 sigma) for the isotope analyses were in the order of $\pm 0.1\text{‰}$ for $\delta^{13}\text{C}_{\text{TC}}$ and
153 $\pm 0.3\text{‰}$ for $\delta^{15}\text{N}$ and $\delta^{34}\text{S}$, as indicated by repeated analyses of samples and standards.

154

155 *3.3 Statistical analysis*

156 The data interpretation was supported by a statistical analysis that was carried out by R (R Core Team,
157 2017). The analysis of variance (ANOVA test) was applied to test if element composition and/or
158 isotopic ratios were affected by the provenance of the sediments. The PCA was applied to examine
159 differences in elemental and isotopic parameters between sediments having Po and Reno affinity
160 (package “FactoMineR” [Le et al., 2008]; package “factoextra” [Kassambara, 2017]).

161 The spatial variation of the various parameters was also investigated. Among the various proxies,
162 the $\delta^{13}\text{C}_{\text{TC}}$ (‰) isotopic signatures appears influenced by the depositional facies, hence a geochemical
163 map was prepared with Q-GIS 3.14.

164

165 **4. Results**

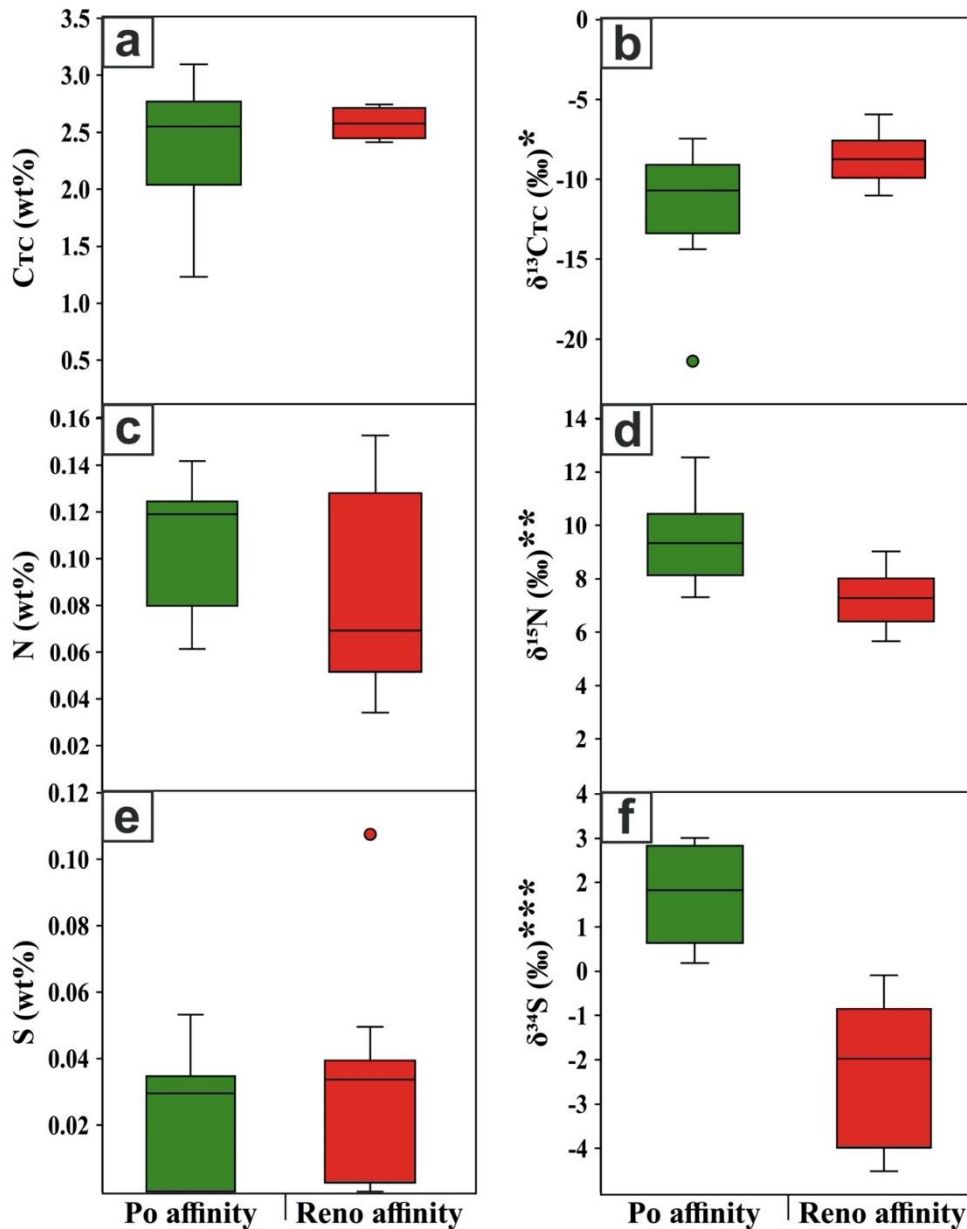
166 The contents of C, N, and S as well as the respective isotopic ratios of alluvial sediments with Po or
 167 Reno River affinity are reported in Table 1.

168

169 **Table 1.** C, N, and S elemental and isotopic composition of alluvial sediments in the surroundings of Ferrara.
 170 Sediments are ascribed to Po and Reno River contributions according to previous studies (Bianchini et al., 2012; 2013).

	Depth (cm)	TC (wt%)	$\delta^{13}C_{TC}$ (‰)	N (wt%)	$\delta^{15}N$ (‰)	S (wt%)	$\delta^{34}S$ (‰)
Po River affinity							
VP3S	30-40	2.81	-10.9	0.13	9.7	0.05	1.9
VP3P	100-120	3.10	-7.5	0.06	9.8	0.04	2.8
VP4S	30-40	2.55	-10.5	0.10	8.9	0.03	3.0
VP5S	30-40	2.76	-14.4	0.14	8.7	0.03	2.6
VP5P	100-120	1.23	-21.4	0.08	7.3	0.03	0.2
VP6S	30-40	2.63	-13.0	0.12	8.1	0.03	2.9
FE25A	30-40	2.04	-12.0	0.12	8.2	< 0.01	0.5
FE25B	100-120	2.55	-8.2	0.08	10.7	< 0.01	0.8
FE29A	30-40	2.48	-9.8	0.12	12.5	< 0.01	1.8
FE29B	100-120	2.04	-9.4	0.12	10.3	< 0.01	0.7
Average		2.42	-11.7	0.11	9.4	0.04	1.7
Reno River affinity							
VM1S	30-40	2.62	-11.0	0.10	6.4	0.04	-2.0
VM1P	100-120	2.58	-7.3	0.05	7.0	0.03	-1.9
VM2S	30-40	2.45	-8.7	0.06	6.3	0.04	-2.6
VM2P	100-120	2.64	-8.0	0.05	6.7	0.05	-4.0
VM3P	100-120	2.71	-9.9	0.07	5.7	0.03	-3.1
VM5S	30-40	2.47	-7.6	0.06	7.6	0.03	-4.1
VM5P	100-120	2.50	-5.9	0.03	9.0	0.03	-1.6
F6P	100-120	2.43	-9.9	0.13	8.0	< 0.01	-0.9
F10S	30-40	2.74	-11.0	0.15	7.3	< 0.01	-0.1
F10P	100-120	2.41	-7.6	0.10	7.8	0.11	-4.5
FE4A	30-40	2.74	-9.2	0.15	9.0	< 0.01	-0.4
Average		2.57	-8.7	0.09	7.3	0.04	-2.3

171 The Total Carbon (TC) concentration of the whole sample population varies between 1.2 and 3.1 wt%
 172 and $\delta^{13}C_{TC}$ ranges from -7.3 to -21.4‰. Significant differences can be observed between sediments
 173 with Po and Reno affinity (Fig. 2a, b).



174
 175 **Figure 2.** Box plots of the C, N, and S elemental and isotopic composition of alluvial sediments in the surroundings of
 176 Ferrara. Sediments are ascribed to Po and Reno River contributions according to previous studies (Bianchini et al., 2012;
 177 2013). For the isotopic parameters, the one-way ANOVA results are also reported (* $p < 0.01$; ** $p < 0.001$; *** $p <$
 178 0.0001), while for the elemental contents, the one-way ANOVA results are not significant.

179 Po River sediments are characterized by TC between 1.2 and 3.1 wt% and $\delta^{13}\text{C}_{\text{TC}}$ between -7.5 and -
 180 21.4‰ with average value of 2.4 wt% and -11.7‰, respectively. Reno River sediments are
 181 characterized by more restricted elemental and isotopic ranges than those of Po River, having TC
 182 between 2.4 and 2.7 wt% and $\delta^{13}\text{C}_{\text{TC}}$ between -7.3 and -11.0‰, with average values of 2.6 wt% and
 183 -8.7‰, respectively. This difference is primarily related to the inorganic and organic carbon (IC and
 184 OC, respectively) ratios, as IC typically has $\delta^{13}\text{C}_{\text{IC}}$ approaching 0‰ and OC typically has very

185 negative $\delta^{13}\text{C}_{\text{OC}}$ down to -25‰ (Natali and Bianchini, 2015). However, our analyses of the distinct
 186 carbon fractions (Table 2) revealed that also OC and IC have distinct isotopic values in Po and Reno
 187 River sediments.

188 **Table 2.** Elemental and isotopic composition of distinct carbon fractions (Organic Carbon, OC; Inorganic Carbon, IC)
 189 of alluvial sediments in the surroundings of Ferrara. Sediments are ascribed to Po and Reno River contributions
 190 according to previous studies (Bianchini et al., 2012; 2013).
 191

	Depth	OC	$\delta^{13}\text{C}_{\text{OC}}$	IC	$\delta^{13}\text{C}_{\text{IC}}$
	(cm)	(wt%)	(‰)	(wt%)	(‰)
Po River affinity					
VP3S	30-40	0.85	-21.8	1.73	-1.2
VP3P	100-120	0.39	-20.5	2.32	-1.5
VP4S	30-40	0.77	-21.1	1.64	-1.4
VP5S	30-40	1.13	-22.0	1.36	-2.2
VP5P	100-120	0.60	-28.1	0.43	-4.1
VP6S	30-40	0.93	-22.4	1.48	-2.7
FE25A	30-40	0.70	-24.5	2.75	-3.3
FE25B	100-120	0.31	-23.6	0.77	-0.4
FE29A	30-40	0.84	-22.8	1.32	0.2
FE29B	100-120	0.56	-22.8	1.32	-0.5
Average		0.71	-23.0	1.51	-1.7
Reno River affinity					
VM1S	30-40	0.75	-22.5	1.59	-0.5
VM1P	100-120	0.43	-21.3	1.98	-0.5
VM2S	30-40	0.48	-22.1	1.72	-1.0
VM2P	100-120	0.49	-22.1	1.88	-1.1
VM3P	100-120	0.34	-20.0	1.86	-0.8
VM5S	30-40	0.54	-20.7	1.88	-0.2
VM5P	100-120	0.63	-21.7	1.92	-0.1
F6P	100-120	0.76	-23.1	1.27	-0.9
F10S	30-40	0.90	-22.7	1.32	-1.5
F10P	100-120	0.50	-22.5	1.53	-1.3
FE4A	30-40	0.80	-22.3	1.80	0.2
Average		0.60	-21.9	1.70	-0.7

192
 193
 194 Samples with Po affinity have on average 0.7 wt% of OC characterized by $\delta^{13}\text{C}_{\text{OC}}$ of -23.0‰ and 1.5
 195 wt% of IC with $\delta^{13}\text{C}_{\text{IC}}$ of -1.7 ‰, whereas those with Reno affinity have on average 0.6 wt% of OC
 196 characterized by $\delta^{13}\text{C}_{\text{OC}}$ of -21.9 ‰ and 1.7 wt% of IC characterized by $\delta^{13}\text{C}_{\text{IC}}$ of -0.7 ‰.

197 The N concentration of the whole sample population varies between 0.03 and 0.15 wt% and $\delta^{15}\text{N}$
198 varies between 5.7 and 12.5 ‰. From the elemental point of view Po and Reno River sediments are
199 indistinct (0.0-0.1 wt%), but they differ in the isotopic composition (Fig. 2 c, d). Po River sediments
200 are characterized by $\delta^{15}\text{N}$ between 7.3 and 12.5‰ with average of 9.4‰, whereas Reno River
201 sediments are characterized by $\delta^{15}\text{N}$ between 5.7 and 9.0‰ with average of 7.3‰. The S
202 concentration of the whole sample population varies from < 0.01 wt% up to 0.11 wt%, whereas $\delta^{34}\text{S}$
203 varies between -4.5 and 3.0‰. Po River sediments are characterized by positive $\delta^{34}\text{S}$ values (between
204 0.2 and 3.0‰, average of 1.7‰), whereas Reno River sediments are characterized by negative $\delta^{34}\text{S}$
205 values (between -4.5 and -0.1‰, average of -2.3 ‰; Fig. 2 e, f).

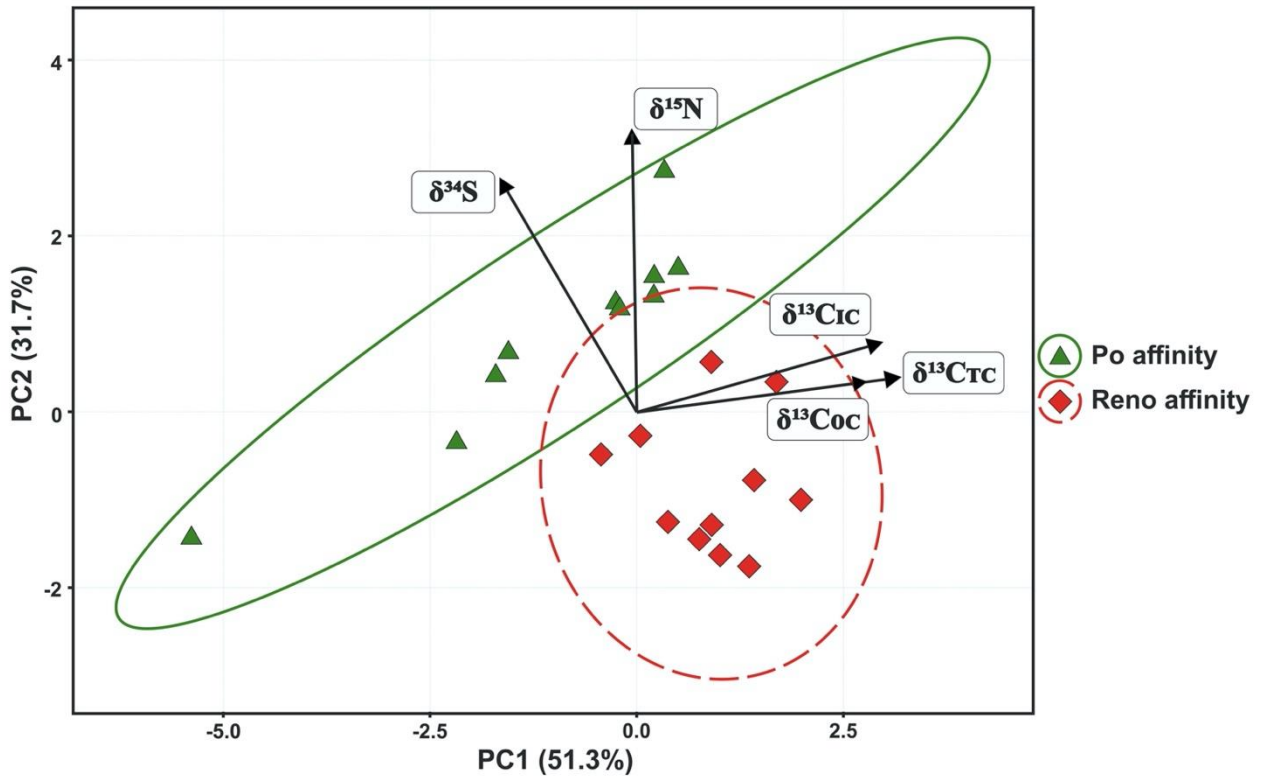
206 The one-way ANOVA test was used to verify if the composition and/or isotopic ratios were affected
207 by the provenance of the sediments (Po or Reno River catchment). The test showed that TC, N, S,
208 OC, IC, and $\delta^{13}\text{C}_{\text{OC}}$ of alluvial sediments were not significantly influenced (p -values > 1) by fluvial
209 system which transported and deposited the sediments on the Padanian Plain. On the other hand, the
210 $\delta^{13}\text{C}_{\text{TC}}$, $\delta^{13}\text{C}_{\text{IC}}$, are moderately affected (p -values < 0.01) by the fluvial system, and $\delta^{15}\text{N}$, $\delta^{34}\text{S}$ are
211 significantly (p -value < 0.001) and extremely (p -value < 0.0001) influenced by the origin of the
212 alluvial sediments, respectively.

213

214 **5. Discussion**

215 The difference between Reno and Po River sediments was already pointed out on the basis of selected
216 trace elements such as Ni and Cr as their high concentration is related to the presence of the ophiolite
217 rock sequences in the Po River hydrological basin and are largely subordinate in the Reno River
218 catchment (Bianchini et al., 2012; 2013, 2019). However, following the ANOVA results and the box
219 plots, the isotopic ratios of C, N, and S are further good parameters to discriminate the sediments for
220 their provenance. Such discrimination is also emphasized by the multivariate statistical analysis
221 (PCA, Fig. 3), where the isotopic ratios of C, N, and S were used as principal components. The PCA

222 plot explains more than 80% of the total variance and well clusters the samples according to the Po
223 and Reno River affinity. In the PCA plot the arrays show a similar length indicating that the isotopic
224 parameters contribute equally to discriminate the two sample populations.

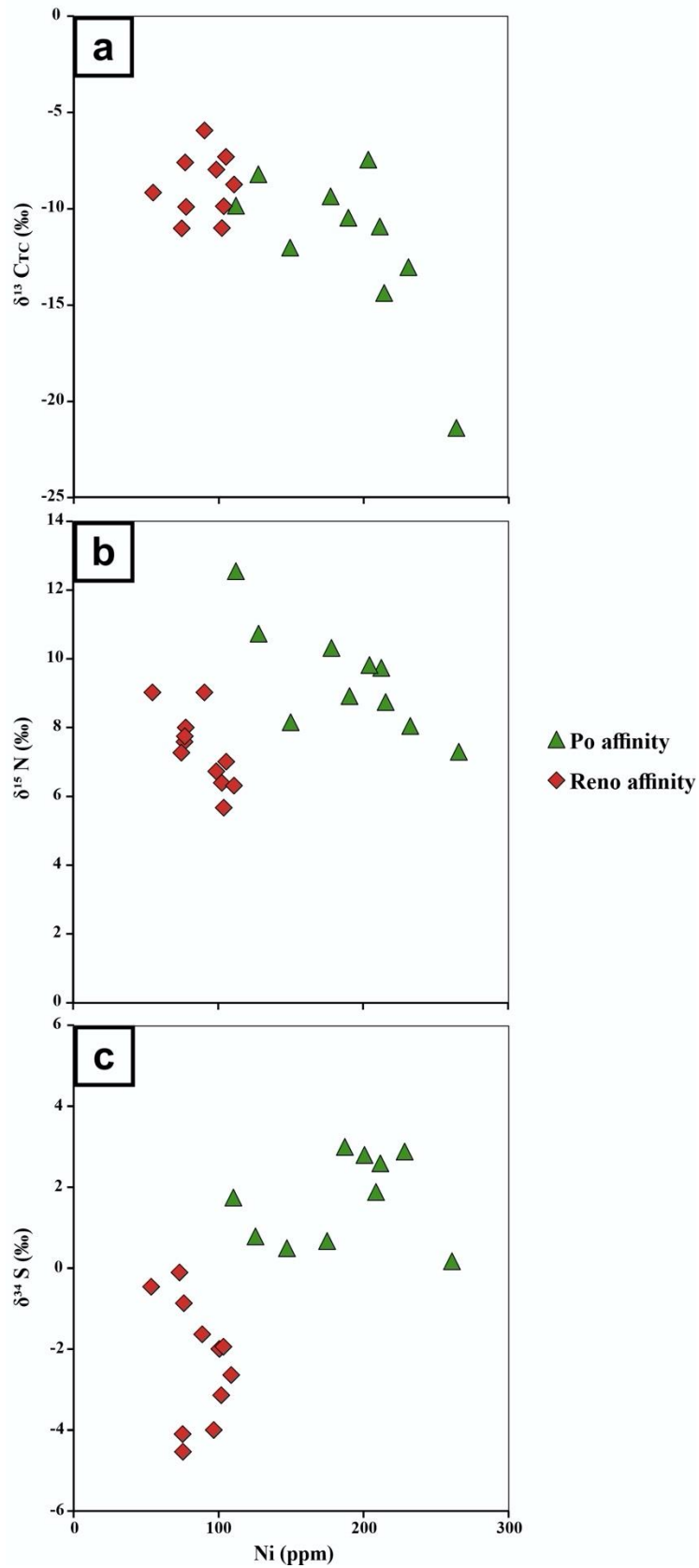


225

226 **Figure 3.** Principal Component Analysis (PCA) for the isotopic ratios of C, N, and S of alluvial sediments in the
227 surroundings of Ferrara having Po and Reno affinity.

228

229 To confirm the significant role of these isotopic tracers in the provenance analysis, $\delta^{13}\text{C}_{\text{TC}}$, $\delta^{15}\text{N}$ and
230 $\delta^{34}\text{S}$ are plotted vs. the Ni content, *i.e.*, the best marker to discriminate between Po and Reno River
231 sediments according to Bianchini et al. (2012; 2013, 2019; Fig. 4). In the biplot diagrams, each
232 isotopic ratio is effective to discriminate the two sample populations.



233

234
235
236

Figure 4. Ni (Bianchini et al. 2012; 2013) vs $\delta^{13}C_{TC}$ (a), $\delta^{15}N$ (b) and $\delta^{34}S$ (c) biplot diagrams discriminate the alluvial affinities in the surroundings of Ferrara from geochemical point of view.

237

238 Hypotheses can be done to explain the reasons for the different C, N, and S isotopic fingerprint on
239 the Po and Reno River alluvial sediments.

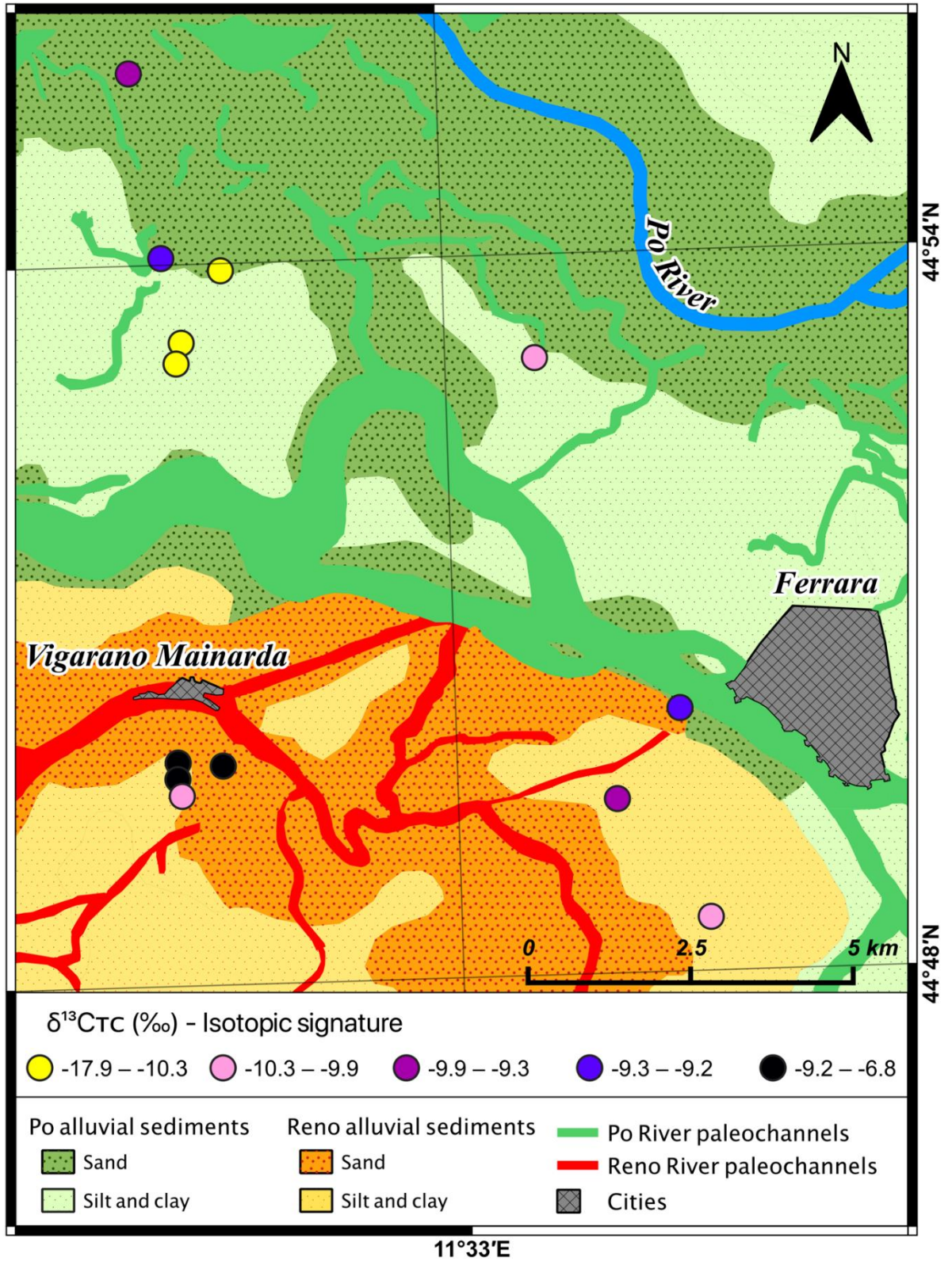
240 For carbon, the TC isotopic fingerprint depends on the OC and IC contents and their relative isotopic
241 ratio. The difference cannot be related to a distinct fertilization history as proposed for other study-
242 cases (Kanstrup et al., 2011) and must be interpreted as a distinctive character of the sediment source
243 area, which is peculiar for every hydrological basin (Li et al., 2020). In general, the $\delta^{13}\text{C}_{\text{OC}}$ is
244 controlled by the distribution of C_3 and C_4 plants, as according to their photosynthetic pathways the
245 $\delta^{13}\text{C}_{\text{TC}}$ ranges from -21‰ and -35‰ for C_3 plants and from -9‰ to -20‰ for C_4 plants (O'Leary,
246 1988; Meier et al., 2014; Brombin et al., 2020). Moreover, in aquatic ecosystems the isotopic
247 composition of the transported organic matter is also influenced by the autochthon growth of biomass
248 constituted by algae and plankton (Finlay and Kendall, 2007).

249 On the other hand, the $\delta^{13}\text{C}_{\text{IC}}$ is controlled by the presence of lithogenic (*i.e.*, primary) or pedogenic
250 (*i.e.*, secondary) carbonates, which have $\delta^{13}\text{C}_{\text{TC}}$ values close to 0‰ or negative, respectively (Gao et
251 al., 2017).

252 Summarizing, the TC isotopic ratios of Po River sediments are generally more negative than those
253 recorded in Reno River sediments (Table 1; Figs. 2b, 4a). This evidence cannot be related to a
254 different proportion of organic and inorganic compounds, because i) the OC and IC contents of Po
255 and Reno River sediments are similar (Table 2) and ii) both $\delta^{13}\text{C}_{\text{OC}}$ and $\delta^{13}\text{C}_{\text{IC}}$ values of Po River
256 sediments are comparatively more negative respect to those of Reno River sediments (Table 2).
257 Indeed, the different distribution of C_3 and C_4 plants could be responsible for the different $\delta^{13}\text{C}_{\text{OC}}$ of
258 the Po and Reno sediments. The Po River hydrological basin comparatively extends at higher latitude
259 and altitude and is plausibly characterized by a higher C_3/C_4 biomass ratio, with respect to the Reno
260 River ratio. Moreover, it has to be noted that, the embankments of Po River are dominated by *Cyperus*
261 vegetation (Pellizzari, 2020), which are C_3 -plants whose $\delta^{13}\text{C}$ signature is extremely negative
262 (Puttock et al., 2012; Lacey et al., 2014; Meier et al., 2014). **In addition**, $\delta^{13}\text{C}$ negativization in

263 suspended particles of Po river water can also be induced by comparatively higher development of
264 fresh water plankton (Søballe and Kimmel, 1987; Finlay and Kendall, 2007). The significant presence
265 of such biomass could be responsible for the more negative $\delta^{13}\text{C}$ signature recorded in the Po River
266 alluvial sediments. In addition, the samples collected in the interfluvial areas of Po River (VP5S,
267 VP5P, VP6S, FE25A) have comparatively negative $\delta^{13}\text{C}_{\text{IC}}$ values, which are indicative of the
268 presence of pedogenic carbonates that enhance the difference of the TC isotopic fingerprint of the
269 two sample populations.

270 Interestingly, the $\delta^{13}\text{C}_{\text{TC}}$ appears effective, not only to discriminate Po and Reno River sediments, but
271 also to precisely constrain the depositional facies. According to the geochemical map of Fig. 5,
272 irrespectively to the provenance of sediments (Po or Reno Rivers catchment), the paleo-channel
273 deposits, mainly composed of sandy sediments, have less negative $\delta^{13}\text{C}_{\text{TC}}$ signature respect to the
274 surrounding interfluvial areas which are mainly composed of clayey sediments. In fact, clays usually
275 form aggregates in which the organic matter remains protected from microbial decomposition, and
276 the organic carbon can therefore preserve its original signature (von Lützow et al., 2006; Gunina and
277 Kuzyakov, 2014; De Clercq et al., 2015; Guillaume et al., 2015).



280 **Figure 5.** Geochemical map of the $\delta^{13}\text{C}_{\text{TC}}$ (‰) showing the distribution of the isotopic signatures near Ferrara and
 281 Vigarano Mainarda.
 282

283 The observed differences on the nitrogen isotopic composition of Reno and Po River sediments can
284 be in principle related to that of the organic matter, but soil $\delta^{15}\text{N}$ value can be also deeply affected by
285 the agricultural practices and the related fertilization history (Bateman and Kelly, 2007; Xu et al.,
286 2012). Noteworthy, in this case-study the observed difference of the two sample populations indicates
287 that the anthropogenic activities did not obliterate the pristine compositions. In fact, the Po River
288 sediments appear to be systematically enriched in ^{15}N with respect to those from the Reno River, a
289 pristine difference of the associated organic matter that generally tends to develop higher $\delta^{15}\text{N}$ as
290 result of the intense biogeochemical transformations (Hobbie and Ouimette, 2009; Craine et al., 2015;
291 Szpak, 2014) occurring in the Po soils which are more mature than those of Reno.

292 The difference on the sulphur isotopic composition of Reno and Po River sediments is also intriguing.
293 As observed for N, the isotopic differences of S could also be explained in terms of soil maturity,
294 since most of soil sulphur should be hosted in the organic matter (*e.g.*, Edwards et al., 1998). In this
295 case, S isotopic fractionation should be controlled by biogeochemical processes producing fugitive
296 gaseous compounds that are generally $\delta^{34}\text{S}$ -depleted (Raven et al., 2015) and leave $\delta^{34}\text{S}$ -enriched
297 residua (Norman et al., 2002). This occurs because during soil biogeochemical processes bacteria
298 preferentially utilize ^{32}S during their metabolism, producing fugitive $\delta^{34}\text{S}$ -depleted products (Strauss,
299 1997). Therefore, as the Po River alluvial soils are more mature than those of Reno River, they
300 developed higher $\delta^{34}\text{S}$ in response to biochemical isotopic fractionation. Noteworthy, among the
301 biogeochemical processes a particular role is represented by sulphate reduction, where anaerobic
302 bacteria reduce the sulphates into sulphides with more negative $\delta^{34}\text{S}$ fingerprint (Guo et al., 2016).
303 This process is associated with the depletion of $\delta^{34}\text{S}$ up to 70‰ in the sediments (Habicht and
304 Canfield, 2001), therefore the produced sulphide is depleted in ^{34}S compared to the sulphate from
305 which is formed. This process could explain the different isotopic signature between the alluvial
306 sediments of the surrounding of Ferrara.

307 On the whole, alluvial soils formed by the deposition of Po River sediments are more mature than
308 those of Reno alluvial soils. This is mainly related to the physiographic difference of the two
309 catchments, as the Po River catchment has a length (652 km) which is four times greater than that of
310 the Reno River catchment (212 km), but also to the timing of sedimentation which appear older for
311 Po River sediments. In fact, locally the interfluvial basins of Po River was definitely reclaimed during
312 the fifteenth century (Bondesan, 1989), whereas the course of Reno River was changed several times
313 until the eighteenth century, when anthropic hydraulic activities defined the actual riverbed
314 (Cremonini, 1989). These different depositional ages are plausibly recorded by the organic matter;
315 Po River soils experienced more complete biogeochemical reactions than that of Reno River
316 sediments. This fact affects the N and S cycles, because as proposed by previous studies organic
317 matter plays a key role in the processes responsible for gaseous loss of nitrogen and sulphur light
318 isotopes (Hobbie and Ouimette, 2009; Norman et al., 2002; Raven et al., 2015).

319

320 **Conclusions**

321 This paper demonstrates that, although intimately associated and interlayered, alluvial sediments
322 having distinct origin show distinct CNS isotope signature. This is validated for alluvial sediments of
323 the easternmost sector of Padanian Plain, where the distinction between Alpine and Apennine
324 contributions (conveyed Po and Reno Rivers, respectively) was known on the basis of heavy metals
325 concentration.

326 We found out that the different CNS isotope fingerprint of Po and Reno River sediments is natural
327 and not induced by anthropogenic anomalies, but doesn't necessarily reflect a lithogenic signature,
328 *i.e.*, it is not solely related to different parent rock types in the Po and Reno River catchments. In fact,
329 we infer that bio-geochemical processes, characterized by distinct ecological conditions in the Po and
330 Reno River catchments, are recorded in the CNS isotopic signatures. Po River sediments are generally
331 few hundreds of years older and pertain to a basin having a path of nearly seven hundred kilometers,
332 much longer than that of Reno River. Consequently, soils developed on Po River sediments are

333 comparatively more mature and record more complete biogeochemical processes that were more
334 intense and affected nitrogen/sulphur compounds generating the distinctive isotope signatures.
335 The important evidence is that the CNS systematics preserve a “memory” of the environment of
336 formation of the conveyed particles, which differs in the distinct basins that feed the alluvial plains.
337 In the considered case-study, this “memory” is not reset by the existing anthropogenic activities.
338 More in general, the reported data increase knowledge on the local elemental and isotopic
339 backgrounds. This is important because many pollutants contain significant CNS concentration and
340 specific isotope composition. Therefore, the presented data will serve as baseline and provide new
341 tools to recognize possible anthropogenic anomalies in the studied area.

342

343 **References**

344

- 345 Amorosi, A. 2012. Chromium and nickel as indicators of source-to-sink sediment transfer in a Holocene
346 alluvial and coastal system (Po plain, Italy). *Sediment. Geol.* 280, 260–269.
347 <https://doi.org/10.1016/j.sedgeo.2012.04.011>.
- 348 Amorosi, A., Barbieri, G., Bruno L., Campo, B., Drexler, T.M., Hong, W., Rossi, V., Sammartino, I.,
349 Scarponi, D., Vaiani, S.C., Bohacs, K.M., 2019. Three-fold nature of coastal progradation during the
350 Holocene eustatic highstand, Po Plain, Italy-close correspondence of stratal character with
351 distribution patterns. *Sedimentology* 66, 3029–3052. <https://doi.org/10.1111/sed.12621>.
- 352 Amorosi, A., Bruno, L., Campo, B., Di Martino, A., Sammartino, I., 2021. Patterns of geochemical
353 variability across weakly developed paleosol profiles and their role as regional stratigraphic markers
354 (Upper Pleistocene, Po Plain). *Palaeogeogr. Palaeoclimatol. Palaeoecol.* 574, 110413.
355 <https://doi.org/10.1016/j.palaeo.2021.110413>.
- 356 Amorosi, A., Centineo, M.C., Dinelli, E., Lucchini, F., Tateo, F., 2002. Geochemical and mineralogical
357 variations as indicators of provenance changes in Late Quaternary deposits of SE Po Plain. *Sediment.*
358 *Geol.* 151, 273–292. [https://doi.org/10.1016/S0037-0738\(01\)00261-5](https://doi.org/10.1016/S0037-0738(01)00261-5).

359 Anderson, D.W., 1988. The effect of parental material and soil development on nutrient cycling in
360 temperate ecosystems. *Biogeochemistry* 5, 71–97.

361 Balabanova, B., Stafilov, T., Sajn, R., Tanaselia, C., 2016. Geochemical hunting of lithogenic and
362 anthropogenic impacts on polymetallic distribution (Bregalnica river basin, Republic of Macedonia).
363 *J. Environ. Sci. Health* 13, 1180–1194. <http://dx.doi.org/10.1080/10934529.2016.1206389>

364 Barbieri, M., Sappa, G., Nigro, A., 2018. Soil pollution: Anthropogenic versus geogenic contributions
365 over large areas of the Lazio region. *J. Geochem. Explor.* 195, 78–86.
366 <https://doi.org/10.1016/j.gexplo.2017.11.014>.

367 Bateman, A.S., Kelly, S.D., 2007. Fertilizer nitrogen isotope signatures. *Isot. Environ. Health Stud.* 43,
368 237–247. <https://doi.org/10.1080/10256010701550732>.

369 Beccaluva, L., Bianchini, G., Natali, C., Siena, F., 2017. The alkaline-carbonatite complex of
370 Jacupiranga (Brazil): Magma genesis and mode of emplacement. *Gondwana Res.* 44, 157–177.
371 <https://doi.org/10.1016/j.gr.2016.11.010>.

372 Bianchini, G., Cremonini, S., Di Giuseppe, D., Gabusi, R., Marchesini, M., Vianello, G., Vittori Antisari,
373 L., 2019. Late Holocene palaeo-environmental reconstruction and human settlement in the eastern Po
374 Plain (northern Italy). *Catena* 176, 324–335. <https://doi.org/10.1016/j.catena.2019.01.025>.

375 Bianchini, G., Cremonini, S., Di Giuseppe, D., Vianello, G., Vittori Antisari, L., 2014. Multiproxy
376 investigation of a Holocene sedimentary sequence near Ferrara (Italy): clues on the physiographic
377 evolution of the eastern Padanian plain. *J. Soils Sediments* 14, 230–242.
378 <https://doi.org/10.1007/s11368-013-0791-2>.

379 Bianchini, G., Di Giuseppe, D., Natali, C., Beccaluva, L., 2013. Ophiolite inheritance in the Po plain
380 sediments: insights on heavy metals distribution and risk assessment. *Ofioliti* 38, 1–14.
381 <https://doi.org/10.4454/ofioliti.v38i1.414>.

382 Bianchini, G., Natali, C., Di Giuseppe, D., Beccaluva, L., 2012. Heavy metals in soils and sedimentary
383 deposits of the Padanian Plain (Ferrara, Northern Italy): Characterisation and biomonitoring. *J. Soils*
384 *Sediments* 12, 1145–1153. <https://doi.org/10.1007/s11368-012-0538-5>.

385 Bertolini, G., Cazzoli, M.A., Centineo, M.C., Cibin, U., Martini, A., 2008. The Geological Landscape
386 of Emilia-Romagna scale 1:250.000. Geological, Seismic and Soil Survey of Emilia Romagna
387 Regional Authority Italy.

388 Bondesan, M., 1989. Evoluzione geomorfologica ed idrografica della pianura ferrarese
389 (Geomorphological and hydrographic evolution of the plain close to Ferrara). In Visser Travagli A.M.
390 and Vighi G. (Eds), Terre ed acqua-Le bonifiche ferraresi nel delta del Po (Land and water - the
391 reclaiming activity in the Po River Delta). Corbo G. publisher, Ferrara (Italy), pp 13–20.

392 Brombin, V., Mistri, E., De Feudis, M., Forti, C., Salani, G.M., Natali, C., Falsone, G., Vittori Antisari,
393 L., Bianchini, G., 2020. Soil carbon investigation in three pedoclimatic and agronomic settings of
394 Northern Italy. Sustainability 12, 10539. <https://doi.org/10.3390/su122410539>.

395 Campo, B., Bruno, L., Amorosi, A., 2020. Basin-scale stratigraphic correlation of late Pleistocene-
396 Holocene (MIS 5e-MIS 1) strata across the rapidly subsiding Po Basin (northern Italy). Quat. Sci.
397 Rev. 237, 106300. <https://doi.org/10.1016/j.quascirev.2020.106300>.

398 Caporale, A.G., Violante, A., 2016. Chemical Processes Affecting the Mobility of Heavy Metals and
399 Metalloids in Soil Environments. Curr. Pollut. Rep. 2, 15–27. [https://doi.org/10.1007/s40726-015-](https://doi.org/10.1007/s40726-015-0024-y)
400 0024-y.

401 Coplen, T. B., Qi, H., 2011. USGS42 and USGS43: Human-hair stable hydrogen and oxygen isotopic
402 reference materials and analytical methods for forensic science and implications for published
403 measurement results. Forensic Sci. Int. 214, 1–3. <http://dx.doi.org/10.1016/j.forsciint.2011.07.035>.

404 Costantini, E.A.C., Angelone, M., Napoli, R., 2002. Soil geochemistry and pedological processes. The
405 case study of the Quaternary soils of the Montagnola Senese (Central Italy). Il Quaternario, Italian
406 Journal of Quaternary Sciences 15, 111–120.

407 Craine, J.M., Brookshire, E.N.J., Cramer, M.D., Hasselquist, N.J., Koba, K., Marin-Spiotta, E., Wang
408 L., 2015. Ecological interpretations of nitrogen isotope ratios of terrestrial plants and soils. Plant Soil
409 396, 1–26. <https://doi.org/10.1007/s11104-015-2542-1>.

410 Cremonini, S., 1989. Morfoanalisi della veteroidrografia centese. Approccio semiquantitativo ad un
411 modello evolutivo del dosso fluviale. Proceedings of the conference “Insediamenti e viabilità
412 nell’Alto Ferrarese dall’età romana all’alto medioevo” Ferrara 135–175.

413 De Clercq, T., Heiling, M., Dercon, G., Resch, C., Aigner, M., Mayer, L., Mao, Y., Elsen, A., Steier, P.,
414 Leifeld, J., Merckx R., 2015. Predicting soil organic matter stability in agricultural fields through
415 carbon and nitrogen stable isotopes. *Soil Biol. Biochem.* 88, 29-38.
416 <https://doi.org/10.1016/j.soilbio.2015.05.011>.

417 Di Giuseppe, D., Bianchini, G., Faccini, B., Coltorti, M., 2014a. Combination of WDXRF analysis and
418 multivariate statistic for alluvial soils classification: a case study from the Padanian Plain (Northern
419 Italy). *X-ray Spectrometry* 43, 165–174. <https://doi.org/10.1002/xrs.2535>.

420 Di Giuseppe, D., Bianchini, G., Vittori Antisari, L., Martucci, A., Natali, C., Beccaluva, L., 2014b.
421 Geochemical characterization and biomonitoring of reclaimed soils in the Po River Delta (Northern
422 Italy): implications for the agricultural activities. *Environ. Monit. Assess.* 186, 2925–2940.
423 <https://doi.org/10.1007/s10661-013-3590-8>.

424 Di Giuseppe, D., Vittori Antisari, L., Ferronato, C., Bianchini, G., 2014c. New insights on mobility and
425 bioavailability of heavy metals in soils of the Padanian alluvial plain (Ferrara Province, northern
426 Italy). *Geochemistry*, 74, 615–623. <https://doi.org/10.1016/j.chemer.2014.02.004>.

427 Dutta, K., Schuur, E.A.G., Neff, J.C., Zimov, S.A., 2006. Potential carbon release from permafrost soils
428 of Northeastern Siberia. *Glob. Chang. Biol.*, 12, 1–16. [https://doi.org/10.1111/j.1365-](https://doi.org/10.1111/j.1365-2486.2006.01259.x)
429 [2486.2006.01259.x](https://doi.org/10.1111/j.1365-2486.2006.01259.x)

430 Edwards, P.J., 1998. Sulfur Cycling, Retention, and Mobility in Soils: A Review. U.S. Department of
431 Agriculture, Forest Service, Northeastern Research Station. 18 p. Doi.: 10.2737/NE-GTR-250

432 Finlay, J.C., Kendall, C., 2007. Stable isotope tracing of temporal and spatial variability in organic matter
433 sources to freshwater ecosystems, In R.H. Michener and K. Lajtha (Eds.), *Stable Isotopes in Ecology*
434 *and Environmental Science*, 2nd edition, Blackwell Publishing, pp. 283–333.

435 Galán, E., González, I., Romero, A., Aparicio, P., 2014. A methodological approach to estimate the
436 geogenic contribution in soils potentially polluted by trace elements. Application to a case study. *J.*
437 *Soils Sediments* 14, 810–818. <https://doi.org/10.1007/s11368-013-0784-1>.

438 Gao, Y., Tian, J., Pang, Y., Liu, J., 2017. Soil inorganic carbon sequestration following afforestation is
439 probably induced by pedogenic carbonate formation in Northwest China. *Front. Plant Sci.*, 8, 1282.
440 <https://doi.org/10.3389/fpls.2017.01282>.

441 Guillaume, T., Damris, M., Kuzyakov, Y., 2015. Losses of soil carbon by converting tropical forest to
442 plantations: erosion and decomposition estimated by $\delta^{13}\text{C}$. *Glob. Chang. Biol.* 21, 3548–3560.
443 <https://doi.org/10.1111/gcb.12907>.

444 Gunina, A., Kuzyakov, Y., 2014. Pathways of litter C by formation of aggregates and SOM density
445 fractions: implications from ^{13}C natural abundance. *Soil Biol. Biochem.* 71, 95–104.
446 <https://doi.org/10.1016/j.soilbio.2014.01.011>.

447 Guo, Q., Zhu, G., Strauss, H., Peters, M., Chen, T., Yang, J., Wei, R., Tian, L., Han, X., 2016. Tracing
448 the sources of sulfur in Beijing soils with stable sulfur isotopes. *J. Geochem. Explor.* 161, 112–118.
449 <https://doi.org/10.1016/j.gexplo.2015.11.010>.

450 Habicht, K.S., Canfield, D.S., 2001. Isotope fractionation by sulfate-reducing natural populations and
451 the isotopic composition of sulfide in marine sediments. *Geology* 29, 555–558.
452 [https://doi.org/10.1130/0091-7613\(2001\)029<0555:IFBSRN>2.0.CO;2](https://doi.org/10.1130/0091-7613(2001)029<0555:IFBSRN>2.0.CO;2)

453 Halas, S., Szaran, J., 2001. Improved thermal decomposition of sulfates to SO_2 and mass spectrometric
454 determinations of $\delta^{34}\text{S}$ of IAEA-SO-5, IAEA-SO-6 and NBS-127 sulfate standards. *Rapid Commun.*
455 *Mass Spectrom.*, 15,1618–1620. <https://doi.org/10.1002/rcm.416>.

456 Hobbie, E.A., Ouimette, P., 2009. Control of nitrogen isotope patterns in soil profiles. *Biogeochemistry*
457 95, 355–371. <https://doi.org/10.1007/s10533-009-9328-6>.

458 Kanstrup, M., Thomsen, I.K., Andersen, A.J., Bogaard, A., Christensen, B.T., 2011. Abundance of ^{13}C
459 and ^{15}N in emmer, spelt and naked barley grown on differently manured soils: towards a method for

460 identifying past manuring practice. *Rapid Commun. Mass. Spectrom.* 25, 2879–2887.
461 <https://doi.org/10.1002/rcm.5176>.

462 Kassambara, F.M., 2017. factoextra: Extract and Visualize the Results of Multivariate Data Analyses. R
463 Package Version 1.0.7. Available online: <https://CRAN.R-project.org/package=factoextra> (accessed
464 on 22 June 2020).

465 Kusaka, S., Nakano, T., 2014. Carbon and oxygen isotope ratios and their temperature dependence in
466 carbonate and tooth enamel using GasBench II preparation device. *Rapid Commun. Mass. Spectrom.*
467 28, 563–567. <https://doi.org/10.1002/rcm.6799>.

468 Lacey, J.P., Olley, J., Pietsch, T.J., Sheldon, F., Bunn, S.E., 2014. Identifying subsoil sediment sources
469 with carbon and nitrogen stable isotope ratios. *Hydrol. Process.* 29, 1956–1971.
470 <https://doi.org/10.1002/hyp.10311>.

471 Le, S., Josse, J., Husson, F. FactoMineR: An R Package for Multivariate Analysis. *J. Stat. Softw.* 2008,
472 25, 1–18. <https://doi.org/10.18637/jss.v025.i01>.

473 Li, S., Xia, X., Zhang, S., Zhang, L., 2020. Source identification of suspended and deposited organic
474 matter in an alpine river with elemental, stable isotopic, and molecular proxies. *J. Hydrol.* 590,
475 125492. <https://doi.org/10.1016/j.jhydrol.2020.125492>.

476 Manzi, V., Roveri, M., Gennari, R., Bertini, A., Biffi, U., Giunta, S., Iaccarino, S.M., Rossi, M.E.,
477 Taviani, M., 2007. The deep-water counterpart of the Messinian Lower Evaporites in the Apennine
478 foredeep: the Fananello section (Northern Apennines, Italy). *Palaeogeogr. Palaeoclimatol.*
479 *Palaeoecol.* 251, 470–499. <https://doi.org/10.1016/j.palaeo.2007.04.012>.

480 Marchina, C., Bianchini, G., Knoeller, K., Natali, C., Pennisi, M., Colombani, N., 2016. Natural and
481 anthropogenic variations in the Po river waters (northern Italy): insights from a multi-isotope
482 approach. *Isot. Environ. Health Stud.* 52, 649–672. <https://doi.org/10.1080/10256016.2016.1152965>.

483 Marchina, C., Bianchini, G., Natali, C., Pennisi, M., Colombani, N., Tassinari, R., Knoeller, K., 2015.
484 The Po river water from the Alps to the Adriatic Sea (Italy): new insights from geochemical and

485 isotopic ($\delta^{18}\text{O}$ - δD) data. *Environ. Sci. Pollut. Res.* 22, 5184–5203. [https://doi.org/10.1007/s11356-](https://doi.org/10.1007/s11356-014-3750-6)
486 [014-3750-6](https://doi.org/10.1007/s11356-014-3750-6).

487 Marchina, C., Natali, C., Fahnestock, M.F., Pennisi, M., Bryce, J., Bianchini, G., 2018. Strontium
488 isotopic composition of the Po river dissolved load: Insights into rock weathering in Northern Italy.
489 *Appl. Geochemistry* 97, 187–196. <https://doi.org/10.1016/j.apgeochem.2018.08.024>.

490 Meier, H.A., Driese, S.G., Nordt, L.C., Forman, S.L., Dworkin, S.I., 2014. Interpretation of Late
491 Quaternary climate and landscape variability based upon buried soil macro- and micromorphology,
492 geochemistry, and stable Isotopes of soil organic matter, Owl Creek, central Texas, USA. *Catena* 114,
493 157–168. <https://doi.org/10.1016/j.catena.2013.08.019>.

494 Natali, C., Bianchini, G., 2015. Thermally based isotopic speciation of carbon in complex matrices: a
495 tool for environmental investigation. *Environmental science and pollution research* 22, 12162–12173.
496 <https://doi.org/10.1007/s11356-015-4503-x>.

497 Natali, C., Bianchini, G., Vittori Antisari, L., 2018. Thermal separation coupled with elemental and
498 isotopic analysis: A method for soil carbon characterisation. *Catena* 164, 150–157.
499 <https://doi.org/10.1016/j.catena.2018.02.022>.

500 Norman, A.L., Giesemann, A., Krouse H.R., Jäger, H.J., 2002. Sulphur isotope fractionation during
501 sulphur mineralization: results of an incubation-extraction experiment with a Black Forest soil. *Soil*
502 *Biol. Biochem.* 34, 1425–1438. [https://doi.org/10.1016/S0038-0717\(02\)00086-X](https://doi.org/10.1016/S0038-0717(02)00086-X).

503 Nyobe, J.M., Sababa, E., Constantin, E., Bayiga, E.C., Ndjiguia P.-D., 2018. Mineralogical and
504 geochemical features of alluvial sediments from the Lobo watershed (Southern Cameroon):
505 Implications for rutile exploration. *C. R. Geosci.* 350, 119–129.
506 <http://dx.doi.org/10.1016/j.crte.2017.08.003>.

507 O’Leary, M.H., 1988. Carbon isotopes in photosynthesis. *Biosciences*, 38, 328–336.

508 Pellizzari, M., 2020. Cyperus-dominated vegetation in the eastern Po river. *Plant Sociol.* 57, 1–16.
509 <http://dx.doi.org/10.3897/pls2020571/06>.

510 Puttock, A., Dungait, J.A.J. Bol, Dixon, E.R., Macleod, C.J.A., Brazier, R.E., 2012. Stable carbon
511 isotope analysis of fluvial sediment fluxes over two contrasting C₄-C₃ semi-arid vegetation
512 transitions. *Rapid Commun. Mass Spectrom.* 26, 2386–2392. <https://doi.org/10.1002/rcm.6257>.

513 R Core Team. R: A language and environment for statistical computing. Available online:
514 <https://www.R-project.org/> (accessed on 22 June 2020).

515 Raven, M.R., Adkinsa, J.F., Werne, J.P., Lyons, T.W., Session, A.L., 2015. Sulfur isotopic composition
516 of individual organic compounds from Cariaco Basin sediments. *Org. Geochem.* 80, 53–59.
517 <https://doi.org/10.1016/j.orggeochem.2015.01.002>.

518 Salomão, G.N., Dall'Agnol, R., Sahoo, P.K., Angélica, R.S., de Medeiros Filho, C.A., da Silva Ferreira
519 Júnior, J., da Silva, M.S., Martins, W. Souza Filho, P., da Rocha Nascimento Junior W., da Costa,
520 M.F., Guilherme, L.R.G., de Siqueira, J.O., 2020. Geochemical mapping in stream sediments of the
521 Carajás Mineral Province: Background values for the Itacaiúnas River watershed, Brazil. *Appl.*
522 *Geochemistry* 118, 104608. <https://doi.org/10.1016/j.apgeochem.2020.104608>.

523 Søballe, D.M., Kimmel B.L., 1987. A Large-Scale Comparison of Factors Influencing Phytoplankton
524 Abundance in Rivers, Lakes, and Impoundments. *Ecology* 68, 1943–1954.

525 Strauss, H., 1997. The isotopic composition of sedimentary sulphur through time. *Palaeogeogr.*
526 *Palaeoclimatol. Palaeoecol.* 132, 97–118. [https://doi.org/10.1016/S0031-0182\(97\)00067-9](https://doi.org/10.1016/S0031-0182(97)00067-9).

527 Szpak, P., 2014. Complexities of nitrogen isotope biogeochemistry in plant-soil systems: implications
528 for the study of ancient agricultural and animal management practices. *Front. Plant Sci.* 5, 288.
529 <https://doi.org/10.3389/fpls.2014.00288>.

530 Vicente, V.A.S., Pratas, J.A.M.S, Santos, F.C.M., Silva, M.M.V.G., Favas, P.J.C., Conde, L.E.N.,
531 2021. Geochemical anomalies from a survey of stream sediments in the Maquelab area (Oecusse,
532 Timor-Leste) and their bearing on the identification of mafic-ultramafic chromite rich complex. *Appl.*
533 *Geochemistry* 126, 104868. <https://doi.org/10.1016/j.apgeochem.2020.104868>.

534 von Lützw, M., Kögel-Knabner, I., Ekschmitt, K., Matzner, E., Guggenberger, G., Marschner, B.,
535 Flessa, H., 2006. Stabilization of organic matter in temperate soils: mechanisms and their relevance

536 under different soil conditions - a review. *Eur. J. Soil Sci.* 57, 426–445.
537 <https://doi.org/10.1111/j.1365-2389.2006.00809.x>
538 Xu, G., Fan, X., Albrecht, K.A., 2012. Plant nitrogen assimilation and use efficiency. *Annual review of*
539 *plant biology* 63, 153–182. <https://doi.org/10.1146/annurev-arplant-042811-105532>.